Heterogeneous Reaction of HOI with Sodium Halide Salts

Juliane C. Mössinger and R. Anthony Cox*

Centre for Atmospheric Science, Department of Chemistry, University of Cambridge, Lensfield Road, Cambridge, CB2 1EW, U. K.

Received: December 12, 2000; In Final Form: February 28, 2001

The interaction of gaseous HOI with crystalline grains of NaCl and sea-salt and thin films of NaBr crystals has been studied in a wall coated tubular flow reactor coupled to a quadrupole mass spectrometer over a concentration range $(0.2-8) \times 10^{12}$ molecules cm^{-3} at 278 and 298 K. On a fresh surface, the uptake coefficients determined were independent of temperature with $\gamma = 0.034 \pm 0.009$, $\gamma = 0.016 \pm 0.004$, and $\gamma = 0.061 \pm 0.021$ for NaBr, NaCl, and sea-salt, respectively. No increase in reactivity was observed on addition of water vapor between 0 and 23% relative humidity at 278 K. It was also shown that the reactivity of the salt surface decreased with time of exposure to HOI and that steady-state uptake was slower on "aged" salt surfaces. Products of the reactions released into the gas phase were IBr, ICl, and IBr + ICl for the reaction of HOI on NaBr, NaCl, and sea-salt surfaces, respectively. The atmospheric implications of the results obtained are briefly discussed.

Introduction

An interest in the tropospheric chemistry of iodine has been developed due to its potential involvement in tropospheric ozone loss.[1−3] The principal known source gases for iodine in the troposphere are alkyl halides emitted from macroalgae and phytoplankton, which can be found in coastal regions as well as in the open oceans.[4−8] Photolysis of alkyl halides produces an iodine atom, which can then react with ozone to form the IO radical, which has recently been observed in three different locations in the remote marine boundary layer.[9,10] The IO radical can then react further with HO_2, NO_2, and IO leading to the formation of a number of inorganic gas-phase species with the major component predicted to be hypoiodous acid, HOI.[2,11]

HOI is formed by the reaction of IO with HO_2 [12]

$$IO + HO_2 \rightarrow HOI + O_2 \qquad (R1)$$

It can then regenerate IO by photolysis[13,14] contributing to ozone destruction via the following reaction cycle[12]

$$HOI + h\nu \rightarrow OH + I \qquad (R2)$$

$$I + O_3 \rightarrow IO + O_2 \qquad (R3)$$

$$IO + HO_2 \rightarrow HOI + O_2 \qquad (R4)$$

HOI can also partition between the gaseous and the condensed phase and undergo heterogeneous reaction with atmospheric aerosol particles. Its uptake into the condensed phase may then lead to removal by wet deposition. Thus, HOI could be the reservoir species responsible for the apparently reversible attachment of I^{131} to aerosol particles, which has been noted during the transport of radioactive material following the accidental release at Chernobyl in 1986.[15,16] In addition, it has recently been proposed that HOI, analogous to HOBr,[17] could also be involved in the activation of halogens from sea-salt aerosols due to formation of interhalogen species, ICl, and IBr[18] via the reactions

$$HOI + NaCl \rightarrow ICl + NaOH \qquad (R5)$$

$$HOI + NaBr \rightarrow IBr + NaOH \qquad (R6)$$

The interhalogens formed are only slightly soluble and can be released back into the gas phase, where they readily photolyze[19]

$$IX + h\nu \rightarrow X + I \ (X = Cl \text{ or } Br) \qquad (R7)$$

The halogen atoms produced could then lead to enhanced ozone loss in the marine boundary layer.

Only one other study of the interaction of HOI with salt surfaces has been published to date. Allanic et al.[20] investigated the reaction of HOI on NaCl and KBr surfaces at room temperature using a Knudsen cell. They reported maximum gamma values for the reactive uptake coefficients of $\gamma = (4 \pm 2) \times 10^{-2}$ and $\gamma = (5 \pm 2) \times 10^{-2}$ for the reaction of HOI on NaCl and KBr respectively, measured at the shortest reaction times. They found that the uptake coefficient decreased with exposure of the salt sample to HOI. The only product observed in their study of the reaction of HOI on NaCl was I_2 but both I_2 and IBr were observed in the reaction of HOI on KBr.

To investigate further the possible release of interhalogens via the reaction of HOI with halide salts, a comprehensive study of the heterogeneous interaction of gaseous HOI with NaBr, NaCl, and sea-salt crystals was conducted using a wall coated flow reactor. The kinetics of HOI uptake on solid NaBr, NaCl, and sea-salt crystals was measured at 298 and 278 K. Uptake measurements were also conducted on a solid NaOH surface and in the presence of water vapor (up to 23% relative humidity at 278 K), to explore the reactivity of the condensed phase product, and the effect of adsorbed water on the reactivity of the solid surfaces. The implications of the resulting uptake coefficients are discussed in terms of the atmospheric chemistry of iodine.

Experimental Section

A conventional flow system with mass spectrometric detection was used to study the uptake kinetics and gaseous reaction

* To whom correspondence should be addressed. Fax: +44-1223-336362. E-mail: jcm34@hermes.cam.ac.uk, rac26@cam.ac.u

10.1021/jp0044678 CCC: $20.00
Published on Web 05/03/2001

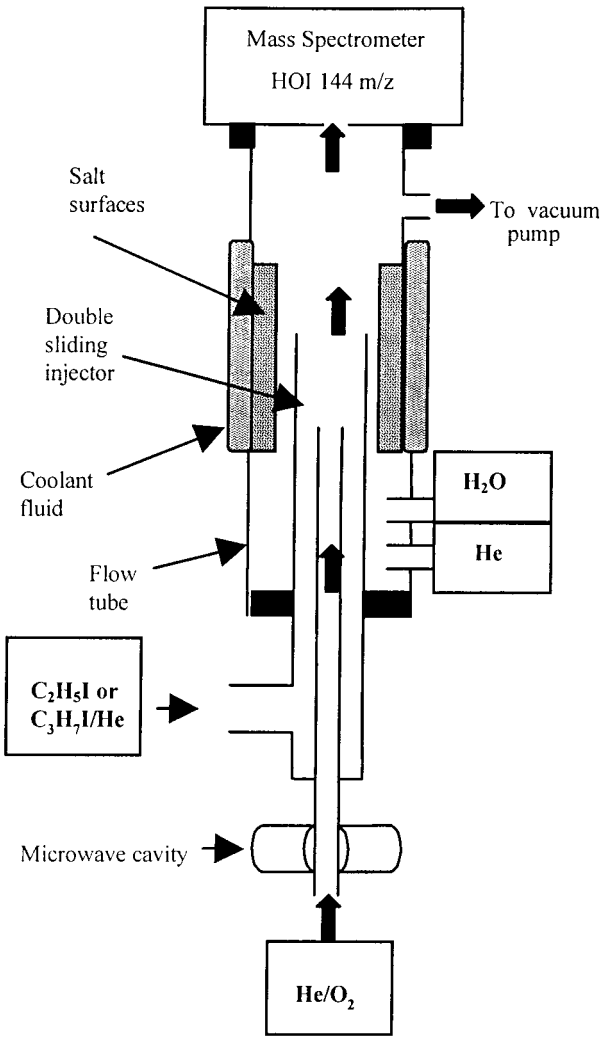

Figure 1. Experimental setup.

products. The apparatus (Figure 1) is similar to that used previously for the study of the interaction of HNO_3 with NaCl and the uptake of HI and HBr on ice,[21,22] except for the double sliding injector, which was used for the in situ preparation of HOI. The jacketed flow tube was approximately 1m in length with an internal diameter of 1.90 cm. A cylindrical Pyrex inner tube 70 cm long and 1.57 cm i.d. was coated internally with the substrate of interest and then inserted inside the flow reactor. This provides the surface for the kinetic measurements.

Two types of surfaces were used in this work. The first type was composed of granular crystallites, which was made using commercial NaCl grains (Breckland Scientific, 99%+) with a diameter of approximately 0.5 mm or sea-salt grains (Community Food Ltd, 99%+) of 0.2−0.7 mm diameter, obtained from solar evaporation of seawater free from any additives or processing aids, deposited in a layer approximately one grain thick. The preparation of this surface type has been described in detail elsewhere.[21] The second type was made in situ by evaporation of a saturated solution of NaBr (Lancaster 99%+) in 50%:50% distilled water/methanol (BDH, 99.8%) or from a 1 molar NaOH solution (Ampules Convol, BDH). To avoid formation of Na_2CO_3, the distilled water used to make up the NaOH solution was boiled prior to use. Once the NaOH solution or the saturated solution of NaBr was made up the inner Pyrex tube insert was immediately coated with it and inserted into the flow reactor. The insert was then dried quickly by pumping out the reactor leaving a slightly opaque thin film of NaOH or NaBr.

TABLE 1: Experimental Conditions for Gases Used

molecule	detection limit/molecules cm^{-3}	concentration/ molecules cm^{-3}	% error
O_2	5×10^{10}	$(0.2-20) \times 10^{13}$	2
C_2H_5I/C_3H_7I	1×10^{11}	$(0.2-20) \times 10^{13}$	5
HOI	2×10^{10}	$(0.2-8) \times 10^{12}$	46
ICl	1×10^{10}	$(2-40) \times 10^{11}$	27
IBr	3×10^{10}	$(2-6) \times 10^{11}$	27
I_2	6×10^{10}	$(7-10) \times 10^{11}$	18

HOI was prepared in situ in the double sliding injector via the reaction of O atoms with C_2H_5I or C_3H_7I[23]

$$O_2 \rightarrow 2\,O(^3P) \qquad \text{(R8)}$$

$$C_xH_yI + O(^3P) \rightarrow HOI + C_xH_{y-1} > 80\% \qquad \text{(R9)}$$

$$C_xH_yI + O(^3P) \rightarrow IO + C_xH_y < 10\% \qquad \text{(R10)}$$

where $x = 2$ or 3 and $y = 5$ or 7 with $k = 2.38 \times 10^{-11}$ cm^3 $molecules^{-1}$ s^{-1} [24] and $k = 5.18 \times 10^{-11}$ cm^3 $molecules^{-1}$ s^{-1} [25] for the reaction with C_2H_5I and C_3H_7I, respectively.

A double sliding injector (see Figure 1) was used in which a flow of O atoms, produced in a microwave discharge of O_2−He mixtures, passed up the inner injector. The O atoms were then mixed a few centimeters before the end of the sliding injector with a flow of excess C_2H_5I or C_3H_7I in He added via the outer injector, which was coated with halocarbon wax. The yield of HOI is in excess of 80%. IO and I_2 were present as small impurities, as detected by mass spectrometry. The resulting HOI concentrations were quite stable in the flow tube. For the study of the reactions of I_2, ICl, and IBr on NaCl, NaBr, sea-salt, and NaOH the double sliding injector was exchanged for a single sliding injector as described previously.[22] Samples of C_3H_7I (Lancaster 98%), C_2H_5I (Lancaster 98%), I_2 (Breckland Scientific 98%), ICl (Lancaster 98%), and IBr (Acros 98%) were purified by repetitive freeze pump thaw cycles. Known pressures of the gases were then mixed with an appropriate pressure of Helium (Messer 5.0) to give the desired percentage mixture (0.01−2%) and stored in bulbs on an all glass manifold. The mixtures were left to mix overnight. They were kept in the dark and usually used the next day. The O_2−He mixture was either used straight from the gas cylinder (O_2 4.5 in He 5%, Messer) or diluted further to the desired percentage mixture of 0.5% in a bulb on the glass manifold.

Gas concentrations were measured using a molecular beam sampling quadrupole mass spectrometer (Hiden Analytical model HAL IV). HOI, IBr, I_2, ICl, C_2H_5I, and C_3H_7I were monitored at m/z = 144, 206, 254, 162, 156, and 171 respectively, using an ionization energy of 70 eV and with a current of 1000 μA. On addition of a flow of a dilute mixture of any of the gases listed above, the mass spectrometer signal was found to be linearly dependent on concentration and calibration curves were obtained for IBr, I_2, ICl, C_2H_5I, and C_3H_7I. Decomposition of some of the ICl and IBr into I_2 and Cl_2/Br_2 was taken into account in the calibrations. The concentration of HOI was determined by subtracting the amount of I_2 formed from the amount of C_2H_5I or C_3H_7I lost assuming that no other iodine containing species were produced when the microwave cavity was switched on. The minimum detectable concentrations, uncertainties in the measured concentrations and typical concentrations used are listed in Table 1. The minimum

TABLE 2: Diffusion Coefficients Used for Brown Corrections

molecule	temp/K	diffusion coeff in He/Torr $cm^2\ s^{-1}$	diffusion coeff in H_2O/Torr $cm^2\ s^{-1}$
HOI	253	224 ± 24.6[27]	33.0 ± 3.6[27]
ICl	278	288.2 ± 31.7	56.6 ± 6.2
IBr	278	268.4 ± 29.5	52.0 ± 5.7.
I_2	278	250.6 ± 7.6	48.0 ± 5.3

reactant concentration used during the experiments was limited to 2×10^{11} molecules cm^{-3} due to the detection limit of 2×10^{10} molecules cm^{-3} for HOI. The initial concentration of HOI has to be sufficiently large to be able to detect changes in the HOI mass signal.

Experiments were performed at 298 and 278 K using a flow of Helium (50−500 sccm) as carrier gas, which was injected through a side inlet at the upstream end of the flow reactor. In the experiments performed at different relative humidity (0−23%), a continuous flow of water vapor was added by either bubbling 150 sccm of Helium through a Pyrex vessel containing high purity water (Acros Organics, water for HPLC) at low pressure or by drawing the water vapor directly from the vessel through another side inlet of the flow reactor. The linear flow velocity varied between 1047 and 2560 $cm^3\ s^{-1}$ and the total pressure of the flow tube was 1.2−3.5 Torr.

For any given experiment, an initial flow of the reactant was established with the end of the sliding injector downstream from the surface of interest. The injector was then moved to an upstream position so that a certain length of the surface was exposed to the reactant. Any uptake on the surface leads to a drop in concentration of the reactant and hence in its signal on the mass spectrometer, and an increase in the product signal, if a product is released into the gas phase. By varying the length of surface exposed the concentration time profile along the flow tube can be determined. Normally, the decay of the reactant was first order and the first-order rate constant $k_{surface}$ can be obtained from a plot of ln[signal] vs contact time. $k_{surface}$ can then be used to calculate the uptake coefficient, γ, assuming that the surface area of the substrate is equivalent to the geometrical surface area of the inner Pyrex tube, using the equation

$$\gamma = k_{surface}\, 2r/\omega \qquad \text{(E1)}$$

where γ = uptake coefficient, ω = average molecular speed and r = radius of the inner Pyrex tube insert.

Corrections for $k_{surface}$ need to be applied for the laminar flow conditions used. The correction for axial diffusion was found to be insignificant (<2%). The correction for radial diffusion was made using the method described by Brown.[26] The diffusion coefficients used for the Brown correction are listed in Table 2. The diffusion coefficients for HOI at 253 K were kindly provided by J. W. Adams[27] prior to publication. For ICl, IBr, and I_2 the diffusion coefficients were calculated using kinetic theory, as described in detail previously.[22] Due to a lack of data for the characteristic energy ϵ and characteristic length σ for IBr in He and H_2O, the diffusion coefficients for IBr were estimated using values of ϵ and σ lying between those for I_2 and ICl.

Uncertainties in temperature, pressure, sample purity, small leaks, gas mixing, slope to determine $k_{surface}$, gas flow, reproducibility of the preparation of surfaces, and the diffusion coefficients used for the diffusion corrections were considered for error analysis. The error attributed to temperature, pressure, sample purity, small leaks, and gas mixing varied between 1 and 5%. The error in the slope to determine $k_{surface}$ was up to 10%, the error for the diffusion coefficients used was 11%. An error of 20% and 30% is assigned to the limited reproducibility of the dried solution surfaces and the salt grain surfaces, respectively. This leads to an overall error on the uptake coefficient of 18%−35%. The correction for radial diffusion using the Brown corrections[26] described above varied between 5 and 60%. They were small when uptake was slow ($\gamma < 10^{-2}$), but became much larger as γ approached 0.1. When $k_{diffusion} < k_{surface}$ the loss of the reactant molecule is limited by the gas-phase diffusion in the flow tube rather then by the reactive uptake onto the surface.[28] Under such conditions only a lower limit for the uptake coefficient can be determined. For all calculations of γ, the geometric surface area of the Pyrex insert was assumed to be equal to the actual surface area available for reaction. Irregularities in the surface may lead to a larger or smaller surface area, as will be discussed later, which would introduce an additional error for the uptake coefficients calculated using equation (E1) above.

Results

I. Interaction of HOI with NaCl, NaBr, Sea-Salt and NaOH Surfaces. *I. (a). Uptake of HOI on Fresh Salt Surfaces.* Figure 2a shows the loss of HOI (1.6×10^{12} molecules cm^{-3}) on NaCl and the production of ICl. The initial HOI signal was established ~2 min after the microwave cavity was switched on. After ~4 min the sliding injector was pulled down to expose the first few centimeters of the surface to HOI and the initial HOI signal decreased to a new steady state value. It can be seen from the increase in ICl signal, that ICl was released promptly into the gas phase. The sliding injector was then repeatedly pulled down to expose different length of the NaCl surface.

On exposure to the NaBr surface HOI (1.1×10^{12} molecules cm^{-3}) was continuously lost to the surface and the product of the reaction, IBr, was released promptly into the gas phase. This is shown in Figure 2b. The sliding injector was pulled back after about 6 min for the first time, and the HOI signal decreased, whereas the IBr signal increased. After 10 min, the microwave cavity was switched off to check the position of the baseline. At 13 min, the cavity was switched back on and the experiment was repeated.

When HOI (1.0×10^{12} molecules cm^{-3}) was lost to the sea-salt surface (Figure 2c)), IBr was observed to be the first product of the reaction reaching the gas phase. The IBr production was found to be time dependent in most cases. At 34 min and 43 min, it can be seen that the initial IBr signal started to decay away almost instantly, while the signal due to ICl production started to increase until it reached a steady-state value. After 51 min, the sliding injector was pushed back up past the sea-salt surface and the HOI signal increased to its initial value, while the ICl signal decreased to its baseline. On fresh surfaces, initial uptake was time dependent, falling from an initial high value to the time independent γ (see Figure 3). However, all values for the uptake coefficient, γ, of HOI on the salt surfaces have been measured after the uptake state had settled to a constant value, as the initial time dependent uptake was not very reproducible. In addition, the maximum change in $k_{surface}$ due to this initial time dependence was a factor of 2, which results in a value for the uptake coefficients within the error limits for the uptake coefficient determined under steady-state conditions. The initial time dependent uptake might become larger when lower concentrations of HOI are used.

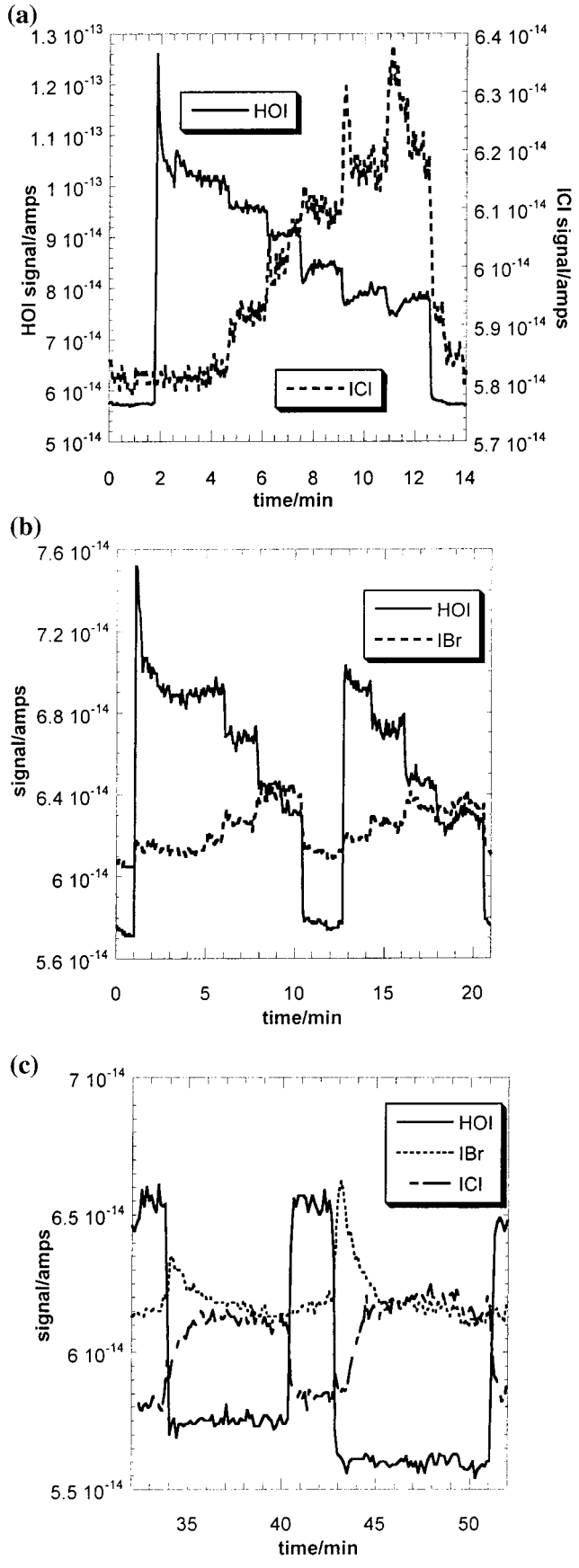

Figure 2. (a) The uptake of HOI (1.6×10^{12} molecules cm^{-3}) on NaCl and the production of ICl at 298 K. (b) The uptake of HOI (1.1×10^{12} molecules cm^{-3}) on NaBr and the production of IBr at 298 K. (c) The uptake of HOI (1.0×10^{12} molecules cm^{-3}) on sea-salt and the production of IBr and ICl at 298 K.

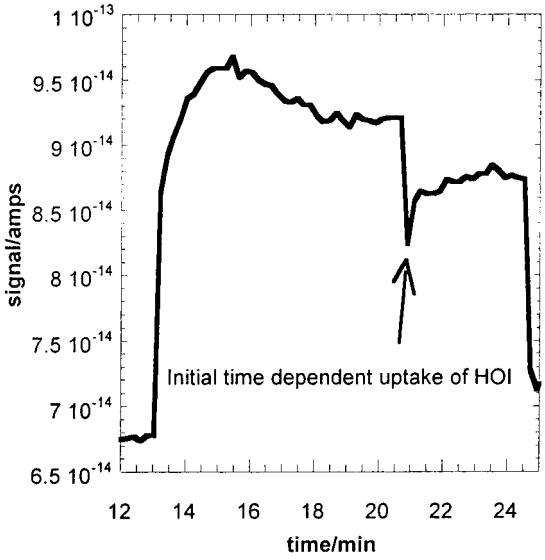

Figure 3. Initial reaction of HOI (1.5×10^{12} molecules cm^{-3}) on a fresh sea-salt surface at 298 K.

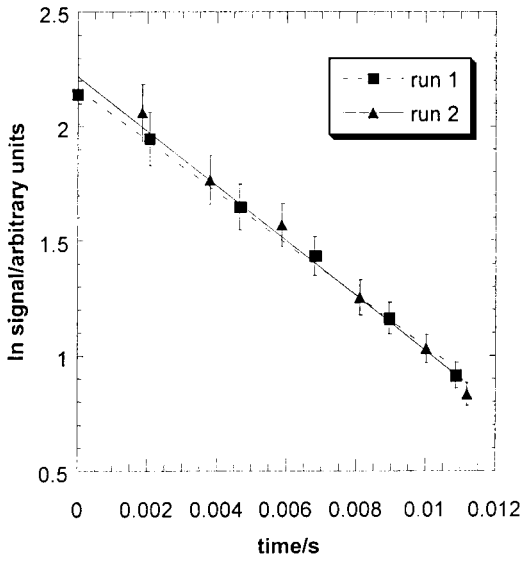

Figure 4. First-order loss plot for the reaction of HOI on sea-salt at 298 K. Two consecutive runs.

Figure 4 shows a typical first-order loss plot for HOI on sea-salt. The two consecutive runs were performed on the same surface.

The uptake coefficients for the loss of HOI on the salt surfaces were found to be independent of temperature between 278 and 298 K with $\gamma = 0.034 \pm 0.009$, $\gamma = 0.016 \pm 0.004$, $\gamma = 0.061 \pm 0.021$ for HOI on NaBr, NaCl, and sea-salt, respectively. The loss of HOI on a clean Pyrex tube insert surface was found to be insignificant with $\gamma = 0.0005 \pm 0.0001$.

I. (b). Surface Aging. It was observed that the reactivity of the dry salt surfaces was dependent on the time of exposure of HOI to the dry salt surfaces. With increasing exposure of HOI to the salt surfaces a decrease in $k_{surface}$ was observed, i.e., γ for the reaction decreased. This behavior, called "surface aging", has also been observed in other studies.[21,20] The measured γ values on "aged" surfaces, e.g., after ~30 min of exposure of the surface to HOI, were determined to be $\gamma = 0.008 \pm 0.003$, $\gamma = 0.007 \pm 0.003$, $\gamma = 0.014 \pm 0.004$ for NaBr, NaCl, and sea-salt, respectively. No concentration dependence of this

surface aging effect was observed over the range of HOI concentration used in this study. However, at lower HOI concentrations, it should be possible to observe a concentration dependence of the effect of surface aging.

I. (c). Effect of Water Vapor. Water was added to the reactor at 278 K up to 23% relative humidity (1.5 Torr water vapor) for the reaction of HOI on NaCl and NaBr and up to 11% relative humidity (0.7 Torr water vapor) for the reaction of HOI on sea-salt. In all cases, no dependence of γ on relative humidity was observed. With the present system, it was not possible to conduct experiments with higher relative humidity in the flow tube. Further increase in water vapor partial pressure would have required an excessive flow tube pressure, to values incompatible with the mass spectrometer sampling configuration. A decrease in orifice size would have resulted in a loss of sensitivity and thus very high initial HOI concentrations, which would have been unsuitable for experiments on dry salt surfaces.

I. (d). Product Formation. For the reaction of HOI on NaCl and NaBr, ICl and IBr, respectively, were the only products detected in the gas phase. Both the loss of HOI as well as the production of ICl and IBr were time independent over the time scale of the experiment. The concentration of ICl produced was calculated to be (10 + 53/−10)% of the concentration of HOI lost to a freshly exposed surface as well as to an "aged" NaCl surface. On a fresh NaBr surface, the amount of IBr produced was calculated to be (100 ± 53)% of the amount of HOI lost. After several experiments carried out on the same NaBr surface the conversion of HOI to IBr decreased to (19 + 53/−19)%. The large errors are mainly due to the uncertainty in the concentration of HOI.

On exposure of HOI to sea-salt both ICl and IBr were observed as products. IBr was observed to be the first product of the reaction reaching the gas phase. Almost instantly, the initial IBr signal started to decay away while the signal due to ICl production started to increase until it reached a steady state value. Thus, IBr and ICl production was time dependent, and at the shortest exposure time on a fresh surface IBr and ICl were produced in a 4:1 ratio. With time the ratio declined and eventually only ICl but no IBr production was observed.

HOI was also found to be taken up on the surface of NaOH, the most likely product of the reaction of HOI on halide salts, which is not released into the gas phase (see section Ie) below). Stoichiometrically, for every IBr or ICl produced there is also OH^- and Na^+ produced on the salt surfaces, which may form the solid reaction product NaOH on the surface. On a medium aged sea-salt surface (30 + 63/−30)% of HOI lost was converted to ICl and IBr. Taking into account that HOI can also be lost to NaOH, (64 ± 63)% of HOI lost could be accounted for. Within error this could close the mass balance for the reactions of HOI on sea-salt. Analysis of the data for the first initial exposure of a fresh sea-salt surface to HOI, i.e., no NaOH present, showed that under these conditions (81 ± 63)% of the HOI lost was converted to ICl and IBr.

I. (e). Interaction of HOI with NaOH. The other possible product of the reaction of HOI on all three salt surfaces was NaOH, which is not likely to be released into the gas phase. To assess the possible interaction of HOI with NaOH, which is assumed to be deposited on an aged surface, the uptake of HOI on an NaOH surface has also been investigated.

The initial reaction rate of HOI upon exposure to a fresh NaOH surface was time dependent, and the uptake coefficient decreased to a steady-state value after the initial exposure. The uptake coefficients reported for the uptake of HOI on an NaOH surface were measured under steady-state conditions for the same reasons as outlined in section Ia. The uptake of HOI (1.4 × 10^{12} molecules cm^{-3}) on NaOH is shown in Figure 5. Between 278 and 298 K, no temperature dependence of the reaction was observed. On a fresh surface, the uptake coefficient was determined to be $\gamma = 0.016 \pm 0.004$. After repeat exposure of HOI to the surface, the value for the uptake coefficient decreased to $\gamma = 0.0022 \pm 0.0006$. No gas-phase products were observed from this reaction. Addition of water vapor at 278 K to 11% relative humidity increased the value for $k_{surface}$ dramatically. Uptake was found to be diffusion-limited with $\gamma \geq 0.1$. As the deliquescence point of NaOH occurs at 7% relative humidity,[29] a solid NaOH surface will change to a liquid layer. Thus, the results suggest that reactivity of HOI on a liquid surface is much greater than on a solid surface.

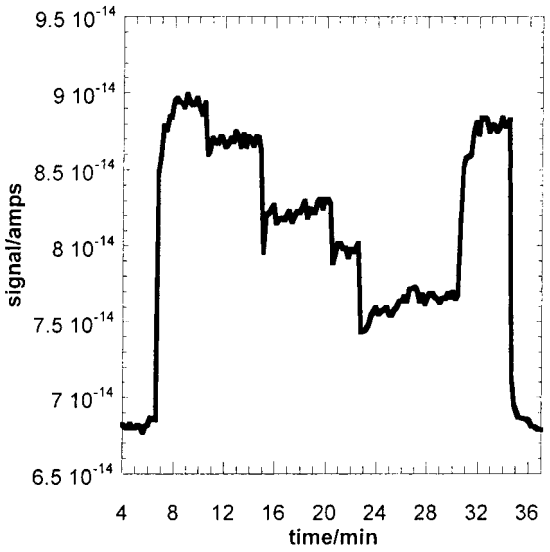

Figure 5. Uptake of HOI (1.4 × 10^{12} molecules cm^{-3}) on NaOH at 298 K.

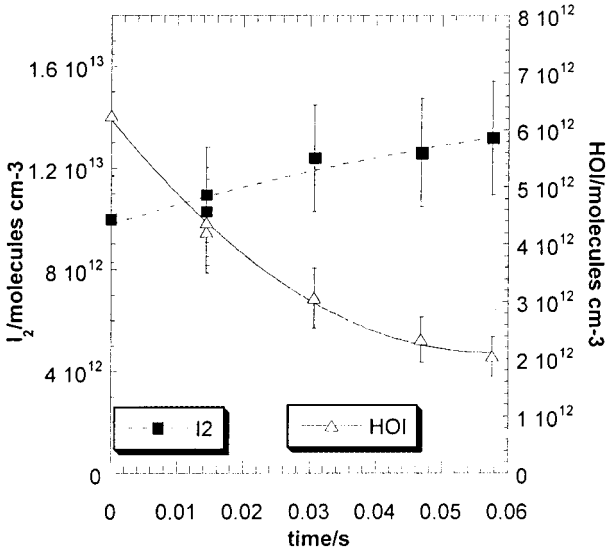

Figure 6. Decomposition reaction of HOI and production of I_2 within the outer sliding injector.

I. (f). Decomposition Reaction of HOI. During the course of the optimization of the HOI source, it was noticed that the HOI signal decreased with increasing length of exposure to the inner wall of the outer sliding injector. At the same time, the I_2 signal increased (Figure 6). This behavior might be explained by the

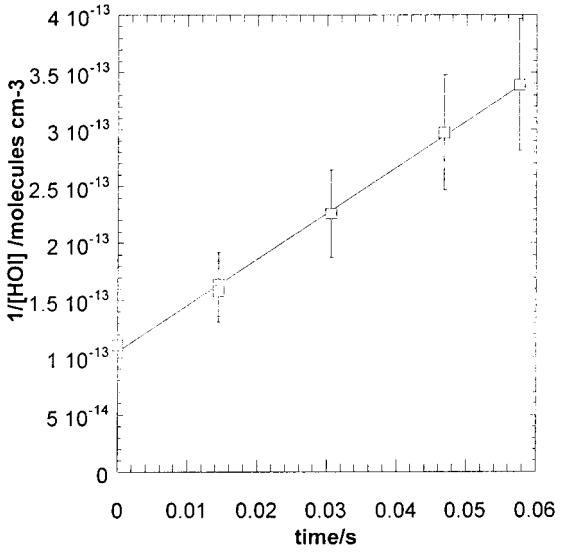

Figure 7. Second-order loss plot for the decomposition of HOI.

following reaction scheme suggesting a decomposition reaction of HOI on the inner wall of the outer sliding injector

$$2\ \mathrm{HOI(g)} \rightarrow 2\ \mathrm{HOI_{(ad)}} \qquad \text{(R11)}$$

$$2\ \mathrm{HOI_{(ad)}} \rightarrow \mathrm{I_2O} + \mathrm{H_2O} \qquad \text{(R12)}$$

$$\mathrm{I_2O} \rightarrow \mathrm{I_2} + 0.5\ \mathrm{O_2} \qquad \text{(R13)}$$

To test the suggested reaction scheme, the data were plotted as a second-order loss plot for the loss of HOI on the walls of the outer injector (Figure 7). No decomposition after dilution in the flow tube was observed.

II. Investigation of the Interaction of ICl, IBr, and I_2 with NaCl, NaBr, Sea-Salt and NaOH Surfaces. To obtain some information about the behavior of the products of the HOI + NaX reaction, the interaction of ICl and IBr with NaX as well as of that of the largest impurity present, I_2, was also studied. No detectable loss of either ICl, IBr, or I_2 on a clean Pyrex insert was observed.

II. (a). ICl, IBr, and I_2 on NaCl and NaBr. No interaction of I_2, ICl, or IBr was observed with the NaCl surface. I_2 and IBr did not interact with the NaBr surface either. In contrast, ICl was lost rapidly to the NaBr surface with production of IBr. The initial rate upon exposure of ICl to a fresh NaBr surface was rapid but time dependent and decreased to a steady state value after approximately 4 min. The uptake coefficient reported for the uptake of ICl on a NaBr surface was measured under steady-state conditions only for the same reasons as discussed in section Ia. The uptake of ICl (3.1×10^{11} molecules cm^{-3}) on NaBr is shown in Figure 8. After 15 min, the first few centimeters of the NaBr surface were exposed to ICl resulting in a decrease of the ICl signal and an increase of the IBr signal. This was repeated several times until, after 47 min, the sliding injector was pushed back past the NaBr surface, and the ICl and IBr signals returned to their initial values. The amount of ICl converted to IBr on a fresh surface was determined to be (100 ± 34)%. However, the conversion decreased to (70 ± 34)% after three consecutive runs on the same NaBr surface indicating some loss of reactivity with exposure to ICl. The initial steady-state uptake coefficient was determined to be $\gamma = 0.0068 \pm 0.0018$.

II. (b). ICl, IBr, and I_2 on Sea-Salt. I_2 did not interact with the sea-salt. On exposure of IBr to the sea-salt surface about

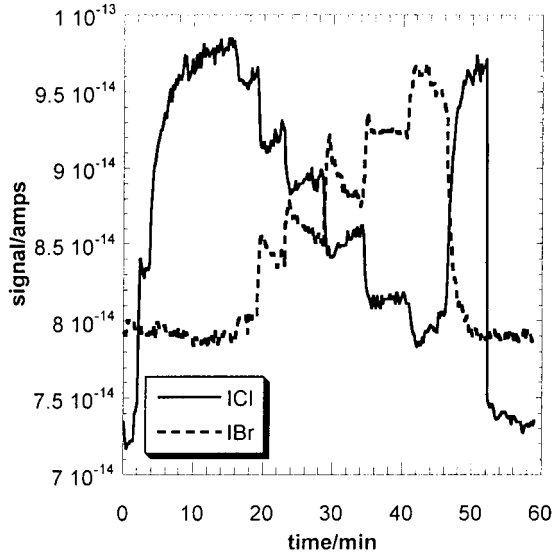

Figure 8. Loss of ICl (3.1×10^{11} molecules cm^{-3}) and production of IBr on a NaBr surface at 298 K.

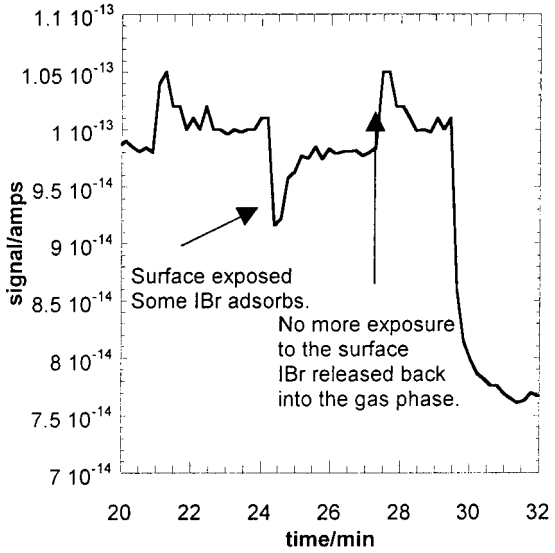

Figure 9. Physical adsorption and desorption of IBr (3.0×10^{11} molecules cm^{-3}) on sea-salt at 298 K.

7% of the initial IBr concentration was lost. No Br_2 or any other gaseous products of the reaction were observed. When the sliding injector was moved back to its initial position so that the surface was no longer exposed to IBr, all the IBr initially adsorbed onto the salt surface was desorbed from the surface again. This physical adsorption process of IBr (3.0×10^{11} molecules cm^{-3}) on sea-salt is shown in Figure 9. The steady-state uptake coefficient was determined to be $\gamma = 0.0006 \pm 0.0002$.

ICl (3.6×10^{11} molecules cm^{-3}) was observed to react with sea-salt as can be seen in Figure 10. After 17, 22, and 29 min increasing lengths of the sea-salt surface were exposed to ICl, which lead to production of IBr. At 34 min, the sliding injector was pushed back up past the sea-salt surface. It was observed that only $(30 + 34/-30)$% of the amount of ICl lost to the surface was converted to IBr, whereas (70 ± 34)% desorbed again as ICl. The reaction was found to be time dependent. After several consecutive experiments on the same sea-salt surface (in this case at 40 min), IBr production was no longer observed and (97 ± 34)% of the ICl lost to the surface

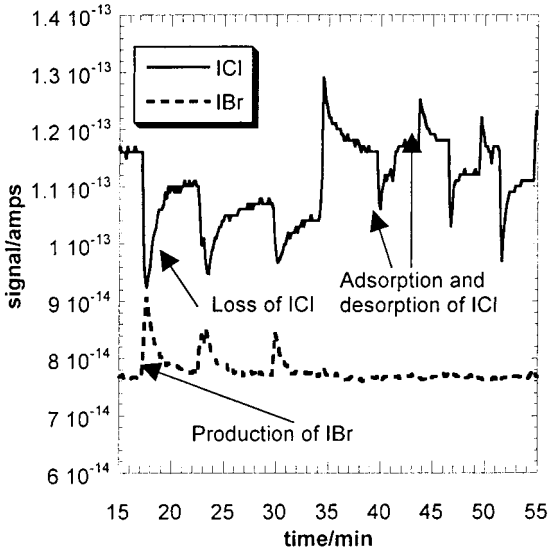

Figure 10. Uptake of ICl (3.6×10^{11} molecules cm^{-3}) on sea-salt: Conversion of ICl to IBr as well as physical adsorption and desorption of ICl from the surface.

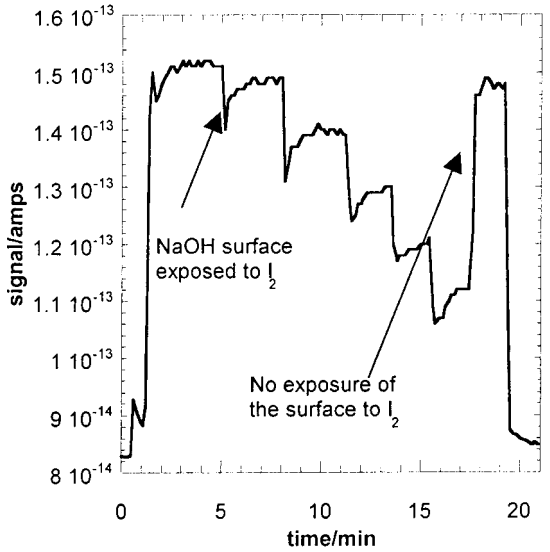

Figure 11. Loss of I_2 (7.6×10^{11} molecules cm^{-3}) on a NaOH surface.

desorbed from it again. $\gamma_{initial}$ was determined to be $\gamma = 0.0012 \pm 0.0004$.

II. (c). ICl, IBr, and I_2 on NaOH. The rates of reaction for I_2, ICl, and IBr on NaOH were all observed to be initially time dependent but decreased quickly to a steady-state value. This is shown for the reaction of I_2 (7.6×10^{11} molecules cm^{-3}) on NaOH in Figure 11. No gas-phase products were observed. The values for gamma were determined to be $\gamma = 0.0045 \pm 0.0012$, $\gamma = 0.0034 \pm 0.0009$, $\gamma = 0.0030 \pm 0.0008$ for I_2, ICl, and IBr, respectively. Between 278 and 298 K, no temperature dependence of the reaction was observed.

On addition of water vapor (11% relative humidity at 278 K), $k_{surface}$ was measured to be much faster and the gamma values increased to $\gamma = 0.016 \pm 0.004$ for I_2 and $\gamma \geq 0.1$ for ICl and IBr. As discussed in section Ie above this result is consistent with the change from the solid NaOH surface to a liquid layer at the higher relative humidity.

A summary of all uptake coefficients measured is shown in Table 3. "No loss" means that it was not possible to detect any loss of the reactant. All γ values reported are an average of at least four experiments.

Discussion

I. Formation of ICl and IBr from the Reaction of HOI on Sea-Salt. It has been shown (results section I, parts a and d) that the uptake of HOI on sea-salt resulted in production of both IBr and ICl. On initial exposure to HOI, IBr was observed to be the first product reaching the gas phase; IBr production then decayed away while ICl grew and was subsequently released continuously to the gas phase, as long as the sea-salt surface was exposed to HOI. Clearly, bromine release is favored over chlorine considering that the composition of sea-salt is 99.5 wt % Cl^- compared to 0.2 wt % Br^-.

The uptake coefficient for HOI on a fresh NaBr surface was determined to be larger than the uptake coefficient for HOI on a fresh NaCl surface. This suggests that the reaction of HOI with Br^- on sea-salt may be more rapid than with Cl^-, leading to preferential release of IBr. However, it was shown (results section IIb) that ICl displayed a stronger chemical and physical interaction with sea-salt than IBr. Therefore, even if ICl is formed competitively with IBr, release of ICl may be slower than IBr leading to an apparently slower reaction

$$HOI + Cl^- \rightarrow ICl_{(ad)} + OH^- \rightarrow ICl_{(g)} + OH^- \quad (R14)$$

$$HOI + Br^- \rightarrow IBr_{(g)} + OH^- \quad (R15)$$

Reaction of ICl with a NaBr surface (see results section IIa) was also observed to form IBr. Thus, even if HOI forms ICl on the sea-salt surface, ICl may be converted to IBr as long as Br^- is available for reaction. ICl is then only released into the gas phase when most of the Br^- on the surface has been depleted

$$HOI + Cl^- \rightarrow ICl_{(ad)} + OH^- \quad (R16)$$

$$ICl_{(ad)} + Br^- \rightarrow IBr_{(g)} + Cl^- \quad (R17)$$

This is similar to the behavior observed by Fickert et al.[30] for the interaction of HOBr and conversion of BrCl to Br_2 in sea-salt solutions. Their observations confirmed experimentally the assumptions made by Huff and Abbatt[31] and Kirchner et al.,[32] who speculated that BrCl was converted to Br_2 on frozen salt solutions as long as there is sufficient Br^- available for surface reaction.

When IBr was exposed to either a NaCl or a sea-salt surface, it did not produce any ICl and showed only a very weak physical interaction with the sea-salt surface. This is consistent with the higher thermodynamic stability of Cl^- compared to Br^- in NaX crystals. The formation of ICl from IBr via the reaction R(18) is therefore unlikely

$$IBr_{(g)} + Cl^-_{(s)} \not\rightarrow ICl_{(g)} + Br^-_{(s)} \quad (R18)$$

II. Decrease in Surface Reactivity—The Effect of Surface "Aging". A decrease in surface reactivity of dry salt surfaces with time of exposure to a reactant molecule has already been observed in many previous studies.[20,21,33] In the present study, a decrease in reactive uptake coefficient was observed with increasing time of exposure of HOI to the substrate. This was attributed to the formation of an involatile product, possibly NaOH, on the surface thus reducing the number of surface halogen ions available for reaction.

It was also shown that HOI reacted with an NaOH surface but uptake was generally slower than on halide salts and no gas-phase products were observed from the reaction. Thus, the fall off in the reaction rate when halide ions are replaced by

TABLE 3: Summary of All Uptake Coefficients Measured

surface	γ HOI	γ ICl	γ IBr	γ I_2
sea-salt/fresh	0.061 ± 0.021	0.0012 ± 0.0004	0.0006 ± 0.0002	No loss
sea-salt/aged	0.014 ± 0.004			
sea-salt/11% RH	0.02 ± 0.007			
NaBr/fresh	0.034 ± 0.009	0.0068 ± 0.0018	no loss	no loss
NaBr/aged	0.008 ± 0.003			
NaBr/11%RH	0.008 ± 0.003			
NaCl/fresh	0.016 ± 0.004	no loss	no loss	no loss
NaCl/aged	0.007 ± 0.003			
NaCl/11%RH	0.008 ± 0.003			
NaOH/fresh	0.016 ± 0.004	0.0034 ± 0.0009	0.0030 ± 0.0008	0.0045 ± 0.0012
NaOH/aged	0.0022 ± 0.0006			
NaOH/11%RH	≥ 0.1	≥ 0.1	≥ 0.1	0.016 ± 0.004
pyrex	0.0005 ± 0.0001	no loss	no loss	no loss

OH^- can be qualitatively accounted for. In solution at high pH, HOI is known to react in the following way[34]

$$HOI + OH^- \rightarrow H_2O + OI^- \qquad (R19)$$

OI^- then reacts further by instantaneous disproportionation[34]

$$3\,OI^- \rightarrow 2I^- + IO_3^-\ K_{dis} = 10^{20} \qquad (R20)$$

With increasing amount of NaOH present, the surface would become progressively basic and HOI could react to form iodide and iodate on the surface. Further reaction to form volatile I_2 would require an acidic surface and is therefore unlikely[34]

$$IO_3^- + 5I^- + 6H^+ \rightarrow 3\,I_2 + 3H_2O \qquad (R21)$$

This would explain the absence of gas-phase products when HOI was lost to the surface. This mechanism also allows, within error, closure of the mass balance for the loss of HOI on an aged salt surface.

ICl, IBr, and I_2 were also observed to undergo reaction with an NaOH surface. Again, no product formation was observed. In basic solution, the following reactions have been observed[34−36]

$$IBr + 2OH^- \rightarrow Br^- + H_2O + OI^- \qquad (R22)$$

$$ICl + 2OH^- \rightarrow Cl^- + H_2O + OI^- \qquad (R23)$$

$$I_2 + 2OH^- \rightarrow I^- + H_2O + OI^- \qquad (R24)$$

OI^- could then react further as described in R20 above.

III. Effect of Water Vapor. If the above reactions known in solution apply to salt surfaces with adsorbed water, an effect of relative humidity might be expected, if the amount of surface adsorbed water was a critical factor. To test the effect of adsorbed water, the relative humidity was increased in several experiments.

Mochida et al.[33] reported that the addition of water vapor did not have an effect on the reaction of HOBr on crystalline NaCl and KBr. They concluded that their negative experimental results meant that there must have been sufficient quantities of adsorbed water on the salt samples already to allow the surface reactions involving ionic species to occur.

Work in this laboratory showed that added water vapor had a significant effect on the uptake rate of HNO_3 on crystalline NaCl surfaces.[21] These surfaces were identical to the NaCl surfaces used in this study of HOI, where no dependence of the uptake rate on water vapor was observed. If the assumption of Mochida et al.[33] was correct, it would mean that the reaction of HOI on NaCl needs a lot less water than the reaction of HNO_3 on NaCl to have the same effect on the uptake coefficient. An alternative explanation is given by the fact that both HNO_3 and HOI form involatile reaction products on the NaCl surface, which may respond differently to the addition of water vapor. For the reaction of HNO_3 on NaCl, the involatile product, $NaNO_3$, is thought to be formed initially as a second layer on the NaCl surface resulting in an aging effect similar to that observed for the reaction of HOI on NaCl. However, the addition of water is thought to result in the formation of a so-called quasi liquid layer[37] on top of the NaCl surface, which leads to precipitation of $NaNO_3$ crystals (deliquescence points for $NaNO_3$, NaCl, and mixtures of NaCl/$NaNO_3$ are 74.3%, 75.3%, and 67.6% relative humidity respectively[38,39]). This precipitation process is thought to rupture the surface structure and expose more Cl^- for reaction with adsorbed HNO_3 [40]. This solid recrystallization process is less likely to happen for NaOH (deliquescence points for NaOH and sea-salt are 7% and 71−75% relative humidity respectively[29]); therefore, restoration by adsorbed water of sites available for reaction may be less efficient, leading to the observed lack of any water vapor effect on the uptake coefficient. These two processes are shown in Figure 12. If this mechanism for the behavior of NaOH on NaCl surfaces is valid, NaOH adsorbed on an NaCl surface must react differently to the addition of water vapor in comparison to the reaction of a pure NaOH surface to the addition of water vapor. The experimental results described in this work (see results section Ie and IIc) showed that addition of water vapor to 11%

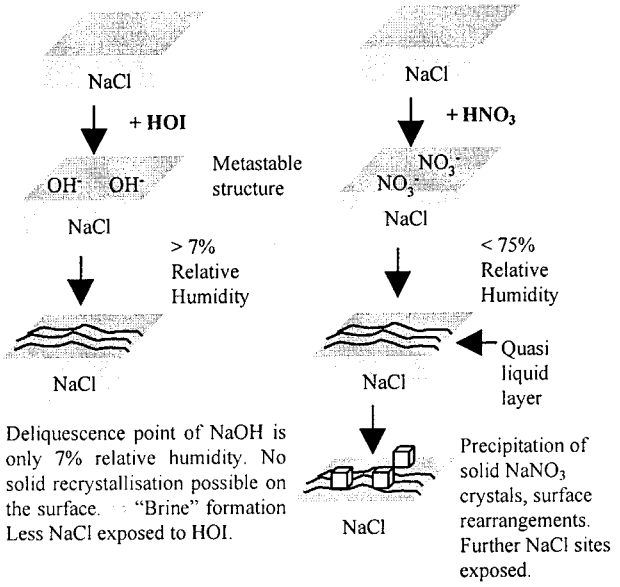

Figure 12. Different behavior of $NaNO_3$ (taken from Laux et al.[40]) and NaOH on the NaCl surface.

relative humidity, i.e., above the deliquescence point for NaOH (7% R. H.), led to a dramatic increase in the rate of reaction for the uptake of HOI, ICl and IBr on a pure NaOH surface. This supports the suggestion that reactions analogous to those in the liquid phase are responsible for reaction on a solid surface. In the case of NaOH adsorbed on a NaCl surface, a large increase in the rate of reaction would only be expected if (a) the deliquescence on this surface occurred at the same relative humidity and (b) it led to newly available surface Cl^- ions.

IV. Extent of Reaction of Br^- and Cl^- in the NaCl, NaBr, and Sea-Salt Samples. To quantify the amount of Br^- and Cl^- available for reaction at the salt surfaces used in this study, the amounts of Br^- and Cl^- present on the top surface layer, based on the geometrical surface area, as well as the total amount of Cl^- and Br^- in the bulk sample were calculated.

The fraction of Br^- in sea-salt is 0.2 wt % or 0.108 mol % and assuming a well mixed salt, the number of Br^- and Cl^- surface sites available at the top surface layer are 6.91×10^{11} cm^{-2} and 6.39×10^{14} cm^{-2}, respectively. The total amount of Br^- and Cl^- available per unit area for reaction can be calculated from the total amount of salt present on the Pyrex tube insert and the geometric area of the surface exposed. The total amount of Cl^- and/or Br^- available was calculated to be $\sim 10^{22}$ molecules cm^{-2}, $\sim 10^{20}$ molecules cm^{-2}, and $\sim 10^{22}$ molecules cm^{-2} (Cl^-)/ $\sim 10^{18}$ molecules cm^{-2} (Br^-) for NaCl, NaBr and sea-salt surfaces, respectively.

The maximum amount of ICl and/or IBr released to the gas phase after reaction of HOI with the NaCl, the NaBr, and the sea-salt surfaces in our experiments was 3×10^{14} molecules cm^{-2}, 1×10^{16} molecules cm^{-2}, and 3×10^{15} molecules cm^{-2} (Cl^-)/2×10^{15} molecules cm^{-2} (Br^-), respectively. It should be noted that the amount of ICl and IBr released was time dependent. Nevertheless, the calculated values showed that in all cases only a small ($\ll$1%) fraction of the total Cl^- and Br^- present in the sample had reacted. However, in the case of NaCl less Cl^- reacted than was present on the top surface layer, whereas for the sea-salt surfaces, in some cases, more Cl^- had reacted than what was present on the top surface layer of the substrate. In the case of NaBr and sea-salt, in most cases, more Br^- had reacted than was present on the top surface layer. This might be due to the fact that a) the "real" surface areas of the NaCl, NaBr, and sea-salt surfaces are different to the assumed geometrical surface areas and/or (b) that the sea-salt was not well mixed and Br^- was concentrated at the surface.

V. Reactivity of the Salt Surfaces Studied. The uptake coefficient for the reaction of HOI on pure NaCl was significantly lower than for HOI on sea-salt. Similarly, de Haan and Finlayson-Pitts[41] observed a lower γ by an order of magnitude for the uptake of HNO_3 on pure NaCl compared to synthetic sea-salt. Behnke and Zetsch[42,43] also reported that reactions generating chlorine atoms are accelerated on sea-salt aerosol relative to NaCl aerosols. A possible explanation for this observation is the increase in the number of defect sites in sea-salt, caused by Br^- dislocations and the presence of mineral salt such as $MgCl_2$.

VI. Geometric Surface Area vs "Real" Surface Area. The correct determination of the actual surface area of salt surfaces available for reaction has been a matter of much debate.[41,44−47] Leu et al.[47,46] applied a model to account for the surfaces of the salt granules beneath the top layer. Other studies[41,44,45,37] claimed that the model is not applicable in all cases and depends not only on the type of surface, but also on the reactant used. For the approximately one grain thick granular salt surfaces used in this study, the model applied by Leu,[46,47] which corrects for interstitial spaces between hexagonal close packed spherical granules stacked in layers, is not appropriate to account for the difference between the geometric surface area and "real" surface area available for reaction. Instead, the approach outlined below has been chosen as an attempt to account for the difference between geometric and "real" surface area available for reaction.

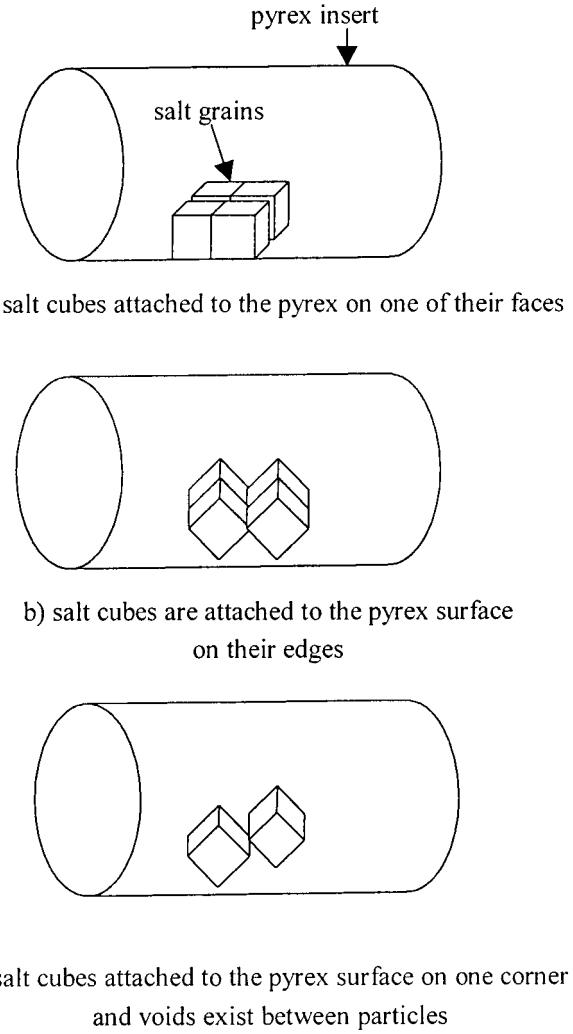

Figure 13. Possible arrangements of salt grains distributed on the cylindrical Pyrex insert.

For the approximately one grain thick granular salt surfaces used in this study the surface area of a simple layer of grains on a surface depends on the arrangements of the grains on the Pyrex tube surface. Figure 13 shows some possible arrangements based on the distribution of the salt grains on the Pyrex insert observed in photomicrographs of the NaCl crystallites taken in this laboratory.[21] Any of the arrangements illustrated in Figure 13 could be representative of the surface. If all the salt grains were attached with one face to the Pyrex surface touching each other without gaps as shown in Figure 13a, the geometric and the real surface area would be approximately equal, i.e., the correction factor is 1. Looking at the photomicrographs most of the NaCl grains appear to be attached to the surface on their edges or corners as shown in Figure 13b−c. As they are distributed all around the glass surface, only the top faces of the crystal cubes have to be considered. If all the salt grains were attached with one edge to the Pyrex surface touching each other without gaps as shown in Figure 13b, the real surface area would be twice the geometric surface area, i.e., the correction factor is 2.

However, so far in both cases, the assumption was made that there are no gaps between the salt particles on the Pyrex surface. This does not appear to be the case looking at the photomicrographs. The porosity, θ, i.e., the fraction of the geometric surface that is void can be calculated from the bulk density, ρ_b (1.13 g cm^{-3}), and the true density, ρ_t (2.165 g cm^{-3}), of NaCl

$$\theta = 1-(1.13 \text{ g cm}^{-3}/2.165 \text{ g cm}^{-3}) = 0.48 \qquad \text{(E2)}$$

This means that, on average, for every salt particle on the surface, there is approximately one void area equivalent to that of one particle on the surface. If the salt cubes are attached to the Pyrex surface on their corners (Figure 13c), all six faces of the cube would be exposed to HOI, but there is only half the number of salt grains distributed on the geometrical surface area if the voids are considered. The maximum correction factor used to obtain the "real surface area" is thus 3.

These simple arrangements do not take into account possible changes in the surface area or reactivity due to defect sites, such as steps and edges, on the surface. The variation of the correction factor from 1 to 3 stresses the importance to work with well characterized substrates. A mean correction factor of 2 ± 1 may be appropriate to apply to the observed γ values for application to the dry sea-salt aerosol.

VII. Comparison with Previous Studies of the Uptake of HOI on Salt Surfaces. Only one other study of the interaction of HOI with salt surfaces has been published to date. Allanic et al.[20] reported values for the uptake coefficient of HOI on NaCl and KBr of $\gamma = (4 \pm 2) \times 10^{-2}$ and $\gamma = (6 \pm 2) \times 10^{-2}$ respectively, which are in good agreement with the values obtained on fresh salt surfaces in this study, considering the experimental uncertainties. Allanic et al.[20] also found that gamma for HOI on KBr decreased with increasing residence time in the Knudsen cell reactor, which is consistent with the surface aging effects reported here.

However, Allanic et al.[20] did not observe production of ICl from the reaction of HOI on NaCl but found I_2 to be the main product. On the KBr surface, I_2 was again the main product with minor amounts of IBr. They concluded that the decomposition of HOI to I_2 was the dominant process, which determined the rate of uptake. In the present study, both ICl and IBr were observed as products of the reaction on NaCl and NaBr, and I_2 was not detected from either reaction. It should be noted that I_2 is one of the major impurities produced as a side product during the in-situ production of HOI. It is therefore difficult to distinguish small changes in the I_2 signal from its large background signal. As described in the results section IV production of I_2 due to decomposition of HOI was only observed within the outer sliding injector, where the concentration of HOI was much higher than that in the flow reactor, hence favoring a second-order surface decomposition reaction. Allanic et al.[20] did not report the concentration of HOI used in their study, but if the concentrations were higher decomposition may well have been the controlling reaction.

VIII. Comparison with the Uptake of HOBr and HOCl on Salt Surfaces. One study for the reaction of HOCl on frozen salt surfaces[31] and four studies of the uptake of HOBr on salt surfaces,[33] frozen salt surfaces,[32] aqueous salt solutions,[30] and deliquescent salt aerosols[50] have been reported in the literature. There are significant differences between the four types of substrates used. The surface of the frozen salt surfaces is generally constantly renewed by water vapor added to the experimental system to inhibit evaporation of the halide−ice surface.[31] The dry salt surfaces undergo an "aging process" e.g., for HOBr uptake.[33] For uptake measurements on aqueous salt solutions and deliquescent salt aerosols, all interactions take place in solution. It should also be noted that HOCl and HOBr are both stronger acids (HOCl > HOBr > HOI with acid dissociation constants being $K_a = 3 \times 10^{-8}$, 2×10^{-9}, 2×10^{-11} respectively[49]), and are more thermally stable molecules compared to HOI.

Huff and Abbatt[31] investigated the reaction of HOCl on frozen bromide−ice, chloride−ice, and bromide/chloride−ice surfaces as a function of temperature and pH of the original solution. At 233 K, a time dependent loss of HOCl on the bromide−ice surface was observed with Br_2 and BrCl being formed as the products of the reaction. The reaction rate was independent of bromine concentration (0.1−1%) at pH < 4. The uptake coefficients reported were $\gamma = 0.051 \pm 0.0013$ at pH 2 and 0.014 ± 0.004 at pH 4−10. These values for the reactive uptake coefficient for HOCl are within error the same as the uptake coefficient for HOI in this study on a fresh NaBr surface and an "aged" NaBr surface, respectively. Surface aging is thought to occur due to poisoning of the dry salt surface possibly by NaOH (see results section Ib and discussion section II, which may have the same effect as changing the pH by adding NaOH to the NaBr solution prior to freezing of halide-ice surfaces.

Huff and Abbatt[31] observed no reaction of HOCl with the chloride−ice surface or the bromide/chloride−ice surface at 233 K, but they observed a loss of HOCl to the bromide/chloride-ice surface at 248 K with production of Br_2 and BrCl. The reaction was observed to be slower ($\gamma = 0.013 \pm 0.004$) than in the experiments with the bromide−ice films. Huff and Abbatt[31] explain this 5-fold change of their gamma value on the bromide/chloride−ice surface compared to the bromide−ice surface with the fact that the chloride physically changes the reactive surface and that thus less Br^- is available for reaction on the surface. The value of their γ is comparable to the uptake coefficient of HOI on an aged sea-salt surface in this study, where the amount of Br^- available for reaction has also been reduced.

Mochida et al.[33] investigated the reaction of HOBr with solid crystalline NaCl and KBr substrates. They observed γ to be time and dose dependent and they quoted values of γ at a vanishing low flow rate of HOBr of $\leq 0.18 \pm 0.04$ for KBr substrates and $\leq (6.5 \pm 2.5) \times 10^{-3}$ for NaCl substrates. The extrapolated value for γ for the reaction of HOBr on NaCl in their study is comparable to the value for the uptake coefficient of HOI on an aged NaCl surfaces in this study. On the other hand, the extrapolated value for γ for the reaction of HOBr on KBr is much larger than the values of γ for the reaction of HOCl, HOBr, or HOI on a NaBr/KBr surface of any other study discussed in this section. This might be explained by the low concentrations used in Mochida et al.'s[33] study (10^9−10^{11} molecules cm^{-3}) compared to all other studies (10^{11}−10^{13} molecules cm^{-3}), but it is not clear why the gamma value should be so different from the one they obtained for NaCl substrates using the same HOBr concentrations.

For HOBr uptake on NaCl substrates Mochida et al.[33] observed Br_2 and BrCl as products of the reaction with a delay in release of BrCl to the gas phase. They suggested that the production of Br_2 originated from the bimolecular self-reaction of HOBr. For the reaction on KBr, they observed Br_2 as the sole product. Mochida et al.[33] also reported a decrease in Br_2 yield from 100% to 50% with increasing HOBr flow rate, which they interpreted as a competition reaction between the heterogeneous reaction of HOBr with NaCl and KBr and the self-reaction of HOBr. A heterogeneous bimolecular self-reaction was also suggested as a possible reaction for HOI by Allanic et

TABLE 4: Summary of Uptake Coefficients for HOI, HOCl, and HOBr on Different Types of Salt Surfaces

author	molecule	surface	pH	conc[a]	aged?	g
this work	HOI	NaBr	−	high	yes	0.008 ± 0.003
this work	HOI	NaCl	−	high	yes	0.008 ± 0.003
this work	HOI	sea-salt	−	high	yes	0.014 ± 0.004
this work	HOI	NaBr	−	low	no	0.034 ± 0.009
this work	HOI	NaCl	−	low	no	0.016 ± 0.004
this work	HOI	sea-salt		low	no	0.061 ± 0.021
allanic	HOI	KBr	−[b]	−	no	0.06 ± 0.02
allanic	HOI	NaCl	−	−	no	0.04 ± 0.02
huff	HOCl	frozen NaBr	low	high	−	0.051 ± 0.0013
huff	HOCl	frozen NaBr	high	high	−	0.014 ± 0.004
huff	HOCl	frozen sea-salt	low	high	−	0.013 ± 0.004
fickert	HOBr	salt solutions	low[c]	-	−	≥ 0.01
kirchner	HOBr	frozen NaBr	−	high	−	0.00327 ± 0.0048
kirchner	HOBr	frozen NaCl	−	high	−	0.00124 ± 0.0047
kirchner	HOBr	frozen sea-salt	−	high	−	0.00142 ± 0.00017
abbatt	HOBr	NaCl aerosol	high	high	−	≤ 0.0015

[a] Low means less than 1×10^{12} molecules cm^{-3}, high means up to 10^{13} molecules cm^{-3}. [b] A dash (−) means not applicable or information not available [c] The uptake was limited by diffusion, and Br_2 release was only observed at low pH not at high pH. The data obtained by Mochida et al.[33] was not included and is discussed in the text.

al.[20] (see discussion section VII) and, in this study, for very high concentrations of HOI present ($\sim 10^{13}-10^{14}$ molecules cm^{-3}) in the outer sliding injector. It is surprising that the HOBr would undergo a self-reaction at the low concentrations used ($10^{9}-10^{11}$ molecules cm^{-3}) by Mochida et al.[33] Abbatt[48] reported in his study of the reaction of HOBr on ice surfaces and HBr/HCl doped ice surfaces that second order kinetics were observed only at concentrations $> 5 \times 10^{12}$ molecules cm^{-3}, which he attributed to the self-reaction of HOBr.

Mochida et al.[33] also speculated that the buildup of involatile bases such as NaOH and KOH may be responsible for a slow decrease of γ with time, which was observed at the higher flow rates of HOBr. This speculation is in agreement with the assumptions made in this work to explain the effect of surface aging (see results section Ie and discussion section II).

Kirchner et al.[32] studied the reaction of HOBr with NaCl, NaBr, and sea-salt doped ice surfaces with $\gamma = (1.24 \pm 0.47) \times 10^{-3}$, $\gamma = (3.27 \pm 0.48) \times 10^{-3}$ and $\gamma = (1.42 \pm 0.17) \times 10^{-3}$ respectively. They observed Br_2 and BrCl as products of the reaction. In comparison with all other data discussed here for HOCl, HOBr and HOI uptake on salt surfaces, their gamma values are surprisingly low and only comparable to the value reported by Abbatt and Waschewsky[50] for the uptake of HOBr on an unbuffered NaCl aerosol. The very high HOBr concentrations (10^{13} molecules cm^{-3}) used in their study might be an explanation for the low gamma values observed, as the surface would become less reactive very quickly.

Abbatt and Waschewsky[50] investigated the heterogeneous interaction of HOBr with deliquescent NaCl aerosols (75% relative humidity) at room temperature. They reported a value for $\gamma \leq 1.5 \times 10^{-3}$, $\gamma \geq 0.2$, and $\gamma \geq 0.2$ for the uptake of HOBr on unbuffered aerosols, aerosols at pH 3 and buffered aerosols at pH 7.2, respectively. Abbatt and Waschewsky[50] explained the strong dependence of the HOBr reactivity on acidity with the rapid depletion of hydrogen ions by the relatively high concentrations of HOBr ($(2-10) \times 10^{12}$ molecules cm^{-3}) used. They reported a lower reactivity at high pH, which is in agreement with the observations made by Huff and Abbatt,[31] Mochida et al.,[33] Fickert et al.,[30] and in this study. However, their reported upper limit for $\gamma \leq 0.0015$ is only comparable to the γ values measured by Kirchner et al.[32] on a frozen NaCl, NaBr and sea salt surface and the reported lower limit for $\gamma \geq (6.5 \pm 2.5) \times 10^{-3}$ for the uptake coefficient for the uptake of HOBr on a dry KBr surface, determined by Mochida et al.[33]

Fickert et al.[30] studied the activation of Br_2 and BrCl via uptake of HOBr onto aqueous salt solutions containing Br^- and Cl^-. They found the reaction to be diffusion-limited with an accommodation coefficient of $\alpha > 0.01$. The uptake coefficient, γ, must thus be larger or equal to 0.01 and this value is comparable to the γ value obtained for HOI on aged sea-salt in this study as well as to the value obtained by Huff and Abbatt[31] for the uptake of HOCl on frozen sea-salt reported above.

Fickert et al.[30] also reported that at a pH of less than 6.5 at least 90% of HOBr taken up was released as gas-phase Br_2. No Br_2 release was observed following HOBr uptake onto nonacidified solution. Similar to what has been reported in the study by Abbatt and Waschewsky,[50] this confirmed the acid catalyzed halogen activation mechanism from sea-salt aerosols predicted by recent models of halogen chemistry in the marine boundary layer.[17,51]

Overall, the three hypohalous acids, HOCl, HOBr, and HOI show a very similar behavior on reaction with salt surfaces. In all cases, the reaction of the hypohalous acid was observed to be faster on Br^- containing surfaces than on Cl^- containing surfaces. For the reaction of both HOBr and HOI on dry salt surface, a surface aging effect was reported.[20,33] In general, for reactions on dry salt surfaces, frozen salt surfaces and deliquescent aerosols a decrease in the values of γ in a more basic surface environment was observed. Within error the γ values for the uptake of HOI, HOCl, and HOBr on the salts determined on fresh surfaces and/or low pH and/or low reactant concentrations ($< 1 \times 10^{12}$ molecules cm^{-3}) were comparable. Similarly, the γ values determined on an aged surface and/or high pH and/or high reactant concentrations ($> 1 \times 10^{12}$ molecules cm^{-3}) were comparable. This is summarized in Table 4. One exception is the very high value ($\gamma \geq 0.2$) obtained for the uptake of HOBr on deliquescent NaCl aerosols at low pH by Abbatt and Waschewsky.[50] This suggests that the γ values obtained for HOI on the dry salt surfaces in this study are likely to be a lower limit for application to marine aerosol particles. To provide a more definite reactive uptake coefficient for atmospheric conditions the uptake of HOI should also be measured on deliquescent sea-salt aerosols.

Atmospheric Implications. The lifetime of HOI with respect to photolysis at midday in the marine boundary layer, for Mace Head, Ireland, July 1997 was calculated to be $\sim$3 min.[52] At the same location and time, the surface-to-volume ratio of the fine fraction of the sea-salt aerosol was determined to be between 50 and 70 μm^2 cm^{-3}.[52] Assuming a value of 60 μm^2 cm^{-3} for

the sea-salt aerosol surface-to-volume ratio and $\gamma = 0.02$ for a loss of HOI on a medium aged aerosol surface, the lifetime of HOI with respect to loss on the aerosol surface was calculated to be ~4 h using the following equations

$$k_{het} = \gamma \frac{\varpi}{4} \frac{S}{V} \quad \text{(E3)}$$

$$\tau = \frac{1}{k_{het}} \quad \text{(E4)}$$

where γ = uptake coefficient for HOI, S/V = the surface-to-volume ratio of the sea-salt aerosol [$cm^2\ cm^{-3}$], ϖ = the average molecular speed [$cm\ s^{-1}$], k_{het} = rate constant for loss on the aerosol [s^{-1}] and τ = the atmospheric lifetime of HOI with respect to loss to sea-salt aerosols [s].

Thus, during the day photolysis is the major loss process for HOI. During night time the uptake on sea-salt becomes the dominant loss process.

The experimental results of this study show clearly that the uptake of HOI on sea-salt leads to the formation of the interhalogen species, ICl and IBr, via the reactions

$$HOI + NaCl \rightarrow ICl + NaOH \quad \text{(R5)}$$

$$HOI + NaBr \rightarrow IBr + NaOH \quad \text{(R6)}$$

The interhalogens formed are only slightly soluble and can be released back into the gas phase, where they readily photolyze[19]

$$IX + h\nu \rightarrow X + I\ (X = Cl \text{ or } Br) \quad \text{(R7)}$$

These reactions are important as two halogen atoms are released into the gas-phase per HOI consumed. The halogen atom concentration in the atmosphere is therefore increased and gas-phase iodine is recycled.

If HOI concentrations in the marine boundary layer were sufficiently large and the heterogeneous reaction with Cl^- and Br^- in the sea salt aerosol was rapid enough, reaction R5−7 might provide a general mechanism for release of reactive Cl^- and Br^- as well as a recycling mechanism for I_X from the marine aerosol (where I_X = total gaseous iodine species). Thus, the marine aerosol would not act as a sink for I_X. The reversible nature of the interaction of gaseous HOI with the salt aerosols could offer a reasonable explanation for the observed behavior of radioactive iodine released to the atmosphere in the accident at the nuclear power plant in Chernobyl in 1986. I^{131} partly remained in gas phase reservoirs and partly in the condensed phase for several days, after release, in an apparent reversible process, leading to enhanced dry deposition in of gaseous I^{131} over a wide region.[15,16]

However, the general mechanism of I_X recycling and Br^- and Cl^- release described above is also strongly dependent on the nature of the salt aerosol. Marine aerosols vary significantly in size and are liquid in most cases. In addition, the HOI concentrations used in this study are several orders of magnitude higher than the atmospheric concentration of HOI (~1 ppt). The measurements performed in this study using high HOI concentrations on solid surfaces are therefore likely to provide a lower limit for the reactive uptake coefficient of HOI on submicron marine aerosol particles.

Conclusions

This study has shown that reaction of gaseous HOI with NaCl, NaBr, and sea-salt occurs with release of gaseous ICl, IBr, and ICl + IBr, respectively. On the sea-salt surface ICl was released into the gas phase with some time delay, which was explained by either conversion of ICl to IBr on the sea-salt surface or a stronger physical interaction of ICl compared to IBr with the sea-salt surface. The effect leading to decreased surface reactivity was attributed to formation of an involatile product of the reaction of HOI on salt, possibly NaOH, on the salt surfaces. The uptake coefficient for HOI on the salt surfaces did not show a dependence on water vapor. It was speculated that this might result from the fact that NaOH, adsorbed on the salt surface, does not recrystallize to free additional surface sites for reaction with Cl^-, as suggested for $NaNO_3$ formed in the reaction of HNO_3 on NaCl.[40] It was also shown that more Br^- was used for the reaction of HOI on NaBr and sea-salt than is available on the top surface layer of the substrate, but much less than is available in total. A correction factor of 2 ± 1 was calculated according to the possible arrangements of salt grains on the surface, which made it possible to correct for the difference in geometric surface area compared to the "real" surface area. The uncertainty in the correction factor highlighted the importance of using well characterized substrates. It was shown that salt aerosols are not likely to be a significant sink for I_X and that Cl^- and Br^- may be released from salt aerosols in the marine boundary layer.

Acknowledgment. The authors thank the U. K. Natural Environmental Research Council for support for this research. We also thank C. J. Percival for help with the double sliding injector setup and with some of the data analysis of preliminary experimental results.

Note Added in Revision

During the course of this work we learned of a similar study on HOI/alkali halide salt interactions conducted at the Max-Planck Institute for Chemistry in Mainz, Germany, which has recently been submitted to *PCCP*. The results of the two studies are in good agreement and show that IBr and ICl are released as reaction products of the interaction of HOI with salt surfaces and not I_2 as previously reported in the literature.

References and Notes

(1) Chameides, W. L.; Davis, D. D. *J. Geophys. Res.* **1980**, *85*, 7383−7393.

(2) Davis, D.; Crawford, J.; Liu, S.; McKeen, S.; Bandy, A.; Thornton, D.; Rowland, F.; Blake, D. *J. Geophys. Res.* **1996**, *101*, 2135−2147.

(3) Jenkin, M. E.; Cox, R. A.; Candeland, D. E. *J. Atmos. Chem.* **1985**, *2*, 359−375.

(4) Carpenter, L. J.; Sturges, W. T.; Penkett, S. A.; Liss, P. S.; Alicke, B.; Hebestreit, K.; Platt, U. *J. Geophys. Res.* **1999**, *104*, 1679−1689.

(5) Klick, S.; Abrahamsson, K. *J. Geophys. Res.* **1992**, *97*, 12 683−12 687.

(6) Laturnus, F.; Wiencke, C.; Kloeser, H. *Mar. Environ. Res.* **1995**, *41*, 169−181.

(7) Schall, C.; Heumann, K. G. *Fresenius J. Anal. Chem.* **1993**, *346*, 717−722.

(8) Singh, H. B.; Salas, L. J.; Stiles, R. E. *J. Geophys. Res.* **1983**, *88*, 3684−3690.

(9) Alicke, B.; Hebestreit, K.; Stutz, J.; Platt, U. *Nature* **1999**, *397*, 572−573.

(10) Allan, B. J.; McFiggans, G.; Plane, J. C. *J. Geophys. Res.* **2000**, *105*, 14,363−14,239.

(11) Jenkin, M. E. *The Photochemistry of Iodine Containing Compounds in the Marine Boundary Layer*; AEA-EE-0405, UKAEA, Harwell Laboratory, 1992.

(12) Wayne, R. P. *Chemistry of Atmospheres*, 2nd ed.; Oxford Science Publications: New York, 1991.

(13) Bauer, D.; Ingham, T.; Carl, S. A.; Moortgat, G. K.; Crowley, J. N. *J. Phys. Chem. A* **1998**, *102*, 2857−2864.

(14) Rowley, D. M.; Mössinger, J. C.; Cox, R. A. *J. Atmos. Chem.* **1999**, *34*, 137−151.

(15) Pacyna, J. M.; Johansen, O.; Salbones, J.; Semb, A. *Air Radioactivity at Selected Stations in Norway after the Chernobyl Reactor Accident*; NILU, 1986.
(16) Clark, M. J.; Smith, F. B. *Nature* **1988**, *332*, 245−249.
(17) Vogt, R.; Crutzen, P. J.; Sander, R. *Nature* **1996**, *383*, 327−330.
(18) Vogt, R.; Sander, R.; Glasow von, R.; Crutzen, P. J. *J. Atmos. Chem.* **1999**, *32*, 375−395.
(19) Seery, D. J.; Britton, D. *J. Phys. Chem.* **1964**, *68*, 2263−2266.
(20) Allanic, A.; Rossi, M. J. *J. Geophys. Res.* **1999**, *104*, 18 689−18 696.
(21) Davies, J. A.; Cox, R. A. *J. Phys. Chem. A* **1998**, *102*, 7631−7642.
(22) Percival, C. J.; Mössinger, J. C.; Cox, R. A. *PCCP* **1999**, *1*, 4565−4570.
(23) Monks, P. S.; Stief, L. J.; Tardy, D. C.; Liebman, J. F. *J. Phys. Chem.* **1995**, *99*, 16 566−16 570.
(24) Loumis, R. A., Klaassen, J. J., Lindner, J., Christopher, P. G.; Leone, S. R. *J. Chem. Phys.* **1997**, *106*, 3934−3947.
(25) Gilles, M. K.; Turnipseed, A. A.; Talukdar, R. K.; Rudich, Y.; Villalte, P. W.; Huey, L. G.; Burkholder, J. B.; Ravishankara, A. R. *J. Phys. Chem.* **1996**, *100*, 14 005−14 015.
(26) Brown, R. L. *J. Res. Nat. Bur. Stand.* **1978**, *83*, 1−8.
(27) Adams, J. W.; MPI-Mainz, Germany, private communication 2000.
(28) Rudich, Y.; Talukdar, R. K.; Imamura, T.; Fox, R. W.; Ravishankara, A. R. *Chem. Phys. Lett.* **1996**, *261*, 467−473.
(29) Twomey, S. *J. Appl. Physics* **1953**, *24*, 1099−1102.
(30) Fickert, S.; Adams, J. W.; Crowley, J. N. *J. Geophys. Res.* **1999**, *104*, 23 719−23 727.
(31) Huff, A. K.; Abbatt, J. P. D. *J. Phys. Chem. A* **2000**, *104*, 7284−7293.
(32) Kirchner, U.; Benter, T.; Schindler, R. N. *Ber. Bunsen-Ges. Phys. Chem.* **1997**, *101*, 975−977.
(33) Mochida, M.; Akimoto, H.; van den Bergh, H.; Rossi, M. J. *J. Phys. Chem. A* **1998**, *102*, 4819−4828.
(34) Adams, C. J.; Downs, A. J. Chlorine, Bromine, Iodine, Astatine. In *Comprehensive Inorganic Chemistry*, 1st ed.; Bailar, J. C.; Emeleus, H. J.; Nyholm, R.; Trotman-Dickenson, A. F., Eds.; Pergamon Press: Oxford, 1973; Vol. 2; pp 1191−1401.
(35) Johnson, D. W.; Margerum, D. W. *Inorg. Chem.* **1991**, *30*, 4845−4851.
(36) Troy, R. C.; Kelley, M. D.; Nagy, J. C.; Margerum, D. W. *Inorg. Chem.* **1991**, *30*, 4838−4845.
(37) Beichert, P.; Finlayson-Pitts, B. J. *J. Phys. Chem.* **1996**, *100*, 15 218−15 228.
(38) Tang, I. N.; Munkelwitz, H. R. *Atmos. Environ.* **1993**, *27*, 467−473.
(39) Tang, I. N.; Munkelwitz, H. R. *J. Appl. Meterol.* **1994**, *33*, 791−796.
(40) Laux, J. M.; Fister, T. F.; Finlayson-Pitts, B. J.; Hemminger, J. C. *J. Phys. Chem.* **1996**, *100*, 19 891−19 897.
(41) de Haan, D. O.; Finlayson-Pitts, B. J. *J. Phys. Chem. A* **1997**, *101*, 9993−9999.
(42) Behnke, W.; Zetzsch, C. *J. Aerosol Sci.* **1990**, *21*, S229−S232.
(43) Behnke, W.; Scheer, V.; Zetzsch, C. *Production of Photolytic Precursors of Atomic Cl from Aerosols and Cl^- in the Presence of Ozone*; Kluwer Academic Publishers: Dordrecht, 1995.
(44) Fenter, F. F.; Caloz, F.; Rossi, M. J. *J. Phys. Chem.* **1994**, *98*, 9801−9810.
(45) Fenter, F. F.; Caloz, F.; Rossi, M. J. *J. Phys. Chem.* **1996**, *100*, 1008−1019.
(46) Leu, M.-T.; Timonen, S. R.; Keyser, F. L. *J. Phys. Chem.* **1995**, *99*, 13 203−13 212.
(47) Leu, M.-T.; Timonen, R. S.; Keyser, F. L. *J. Phys. Chem. A* **1997**, *101*, 278−282.
(48) Abbatt, J. P. D. *Geophys. Res. Lett.* **1994**, *21*, 665−668.
(49) Greenwood, N. N.; Earnshaw, A. The Halogens. In *Chemistry of the Elements*, 1st ed.; Pergamon Press: Oxford, 1994.
(50) Abbatt, J. P. D.; Waschewsky, G. C. G. *J. Phys. Chem. A* **1998**, *102*, 3719−3725.
(51) Sander, R.; Crutzen, P. J. *J. Geophys. Res.* **1996**, *101*, 9121−9138.
(52) McFiggans, G.; Plane, J. M. C.; Allan, B. J.; Carpenter, L. J.; Coe, H.; O'Dowd, C. *J. Geophys. Res.-Atmos.* **2000**, *105*, 14 363−14 369.